

Aboveground Biomass Estimation of Rice Crops (*Oryza sativa* L.) Utilizing Parameters Derived From UAV-Based LiDAR And Multispectral Satellite Sensors

Chelsea L. Gadrinab¹, Jasper Joaquin S. Israel¹, Ayin M. Tamondong¹, Roel T. Bahia¹

¹Department of Geodetic Engineering, University of the Philippines, Diliman, Quezon City, Philippines –
(clgadrinab, jsisrael, amtamondong, rtbahia)@up.edu.ph

Keywords: aboveground biomass, rice, canopy height, canopy cover, vegetation indices.

Abstract

This study investigates efficient, non-destructive approaches for estimating rice aboveground biomass (AGB), a key yield indicator. It integrates Unmanned Aerial Vehicle - based Light Detection and Ranging (UAV-LiDAR) sensor for structural data and multispectral satellite imagery for spectral data to develop individual and fused models aimed at improving AGB estimation accuracy. Data were collected across three rice growth stages during one planting season for National Seed Industry Council (NSIC) Rc 222 and NSIC Rc 160 rice cultivars, using UAV-LiDAR, PlanetScope imagery, and field-based AGB measurements, wherein 30 samples were used for analysis. Multiple linear regression was used to model fused spectral and structural parameters for each variety. Results showed model performance depends on rice variety. Through Leave-One-Out Cross-Validation (LOOCV) and the corrected Akaike Information Criterion (AICc), the spectral-only model for NSIC Rc 160 using Green Normalized Difference Vegetation Index (GNDVI) performed best ($R^2=0.62$, RMSE=5.16, rRMSE=1.85%, AICc=187.10). Structural data did not improve the model. For NSIC Rc 222, the fused model combining GNDVI, Normalized Difference Yellowness Index (NDYI), and canopy height achieved the highest accuracy ($R^2 = 0.82$, RMSE=10.40, rRMSE=5.86%, AICc=165.60), indicating that combining spectral and structural data enhances predictions. Due to the small sample size, LOOCV was used, but larger datasets are needed to explore advanced machine learning methods. These findings support modeling approaches per rice variety and highlight its potential for precision agriculture applications in rice biomass estimation.

1. Introduction

Rice is a vital staple food for more than half of the global population (Fukagawa and Ziska, 2019). Despite having a tropical climate that supports year-round cultivation, the Philippines remains heavily reliant on rice import due to high domestic demand as a cultural mainstay, consumed with most meals. Accurate methods for estimating rice yield have become increasingly important in ensuring food security in the face of environmental and economic pressures.

One of the most important indicators of rice crop performance is aboveground biomass (AGB), which refers to the dry weight of all crop material above the soil surface. Traditionally, AGB has been estimated through destructive sampling methods that involve selecting sample rice plants and oven-drying until constant weight (Zheng et al., 2019; Mansaray et al., 2020). While this approach yields accurate results, it is labor-intensive, time-consuming, and can lead to crop loss, making it impractical for large-scale or frequent monitoring (Ndikumana et al., 2018).

To address these limitations, remote sensing technologies allow for detailed spatial and temporal data on crop health and growth, covering large areas with minimal manual labor. Two promising methods are Light Detection and Ranging (LiDAR) and multispectral imaging. LiDAR can detect early signs of crop stress and monitor changes in plant structure, making it useful for timely yield forecasting and management interventions (Farhan et al., 2022). Multispectral imaging, on the other hand, captures data across various wavelengths to assess plant health. Vegetation indices are helpful during vegetative and reproductive phases, when rice plants are most vulnerable to environmental stressors, pests, and nutrient deficiencies (Sergieieva, 2024).

The combination of LiDAR and multispectral imaging offers a comprehensive approach to biomass estimation by integrating both structural and spectral data. Research has shown that combining these datasets can enhance the accuracy of yield predictions (Wan et al., 2020; Khodjaev, 2023), yet there remains limited investigation into their combined use for rice AGB estimation specifically. Hence, the objectives of the study are to extract structural parameters from Unmanned Aerial Vehicle or UAV-based LiDAR data, derive spectral parameters from multispectral satellite imagery, develop individual AGB estimation models based on each data source, and construct a combined model using both spectral and structural inputs to assess accuracy and reliability in estimating rice aboveground biomass.

2. Methodology

2.1 Data Acquisition

The study observed two rice cultivars, National Seed Industry Council (NSIC) Rc 222 and NSIC Rc 160 during one planting season. These varieties were cultivated in two 1,200-square meter controlled experimental rice plots, as shown in Figure 1, located at the University of the Philippines- Los Baños, which received different fertilizer treatments.

Data were collected during three key growth stages: tillering, panicle initiation, and booting or heading, corresponding to the vegetative and reproductive phases of rice growth. LiDAR data were obtained from UAV-LiDAR using a LiAir X3C-H sensor mounted on a PPTI-ENT M410 drone flown at a 20-meter altitude in 3m/s, maintaining a 40% sidelap at stable light conditions. The UAV-LiDAR system generated point cloud data with a ground sampling resolution of approximately 5 cm, which was later processed to derive canopy height and cover. On the contrary, multispectral satellite data were obtained from PlanetScope 8-band surface reflectance imagery, which

provides a 3-meter spatial resolution, acquired within three days of each field campaign to minimize temporal variation. Field data for validation included plant height, tiller count, and aboveground biomass, collected through systematic sampling in 0.5 by 0.5 meter plots across both rice fields. Rice samples, consisting of eight rice hills, were harvested, cleaned, and oven-dried for 72 to 120 hours, to determine dry weight. For this research a total of 30 samples were collected, with 15 samples per rice variety.

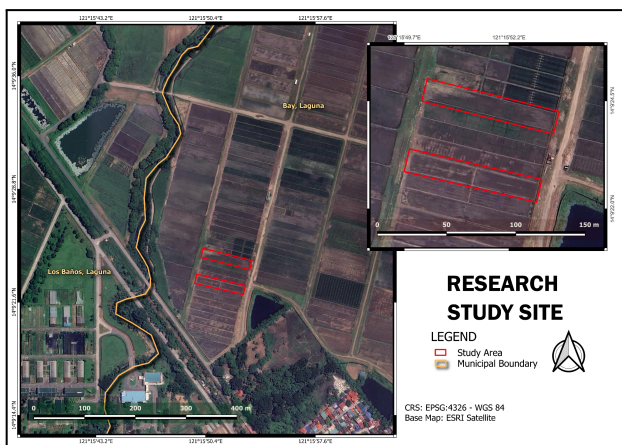


Figure 1. Study Area

Table 1 below shows the schedule of data acquisition in Days After Transplanting (DAT) for each type of dataset obtained.

Data Acquisition Type	Growth Stages (DAT, Date)		
	Tillering Stage	Panicle Initiation Stage	Booting & Heading Stage
NSIC Rc 222			
LiDAR	45th day March 12, 2025	70th day April 05, 2025	77th day April 12, 2025
Satellite	46th day March 13, 2025	67th day April 02, 2025	74th day April 09, 2025
Field	49th day March 15, 2025	70th day April 05, 2025	77th day April 12, 2025
NSIC Rc 160			
LiDAR	33rd day March 12, 2025	58th day April 05, 2025	65th day April 12, 2025
Satellite	34th day March 13, 2025	55th day April 02, 2025	62nd day April 09, 2025
Field	37th day March 15, 2025	58th day April 05, 2025	65th day April 12, 2025

Table 1. Data Acquisition Sessions

2.2 Data Processing

The raw LiDAR data were georeferenced using Position and Orientation System (POS) processing with RINEX files from a continuous GNSS observation to correct horizontal and vertical positions based on known ground control points. A sample pre-processed colorized LiDAR point cloud and its corresponding profile view is shown Figure 2. Moreover, PlanetScope images were also georeferenced using observed semi-permanent ground points. This ensures spatial consistency across all the datasets.

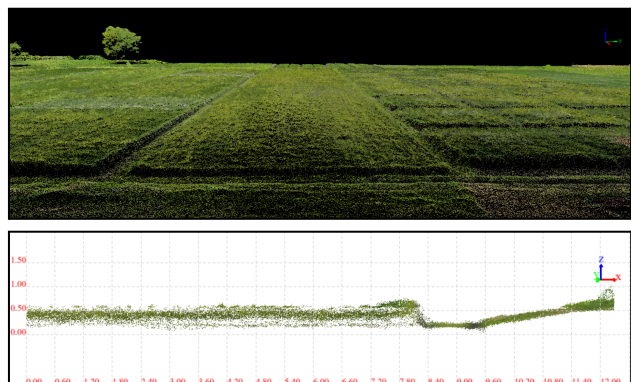


Figure 2. Colorized point cloud of NSIC Rc 222 plot in one data acquisition phase (77 Days After Acquisition)

2.2.1 Canopy Height: To obtain the canopy heights, Digital Elevation Models (DEM) to represent the ground and the Digital Surface Models (DSM) to represent the canopy were created for each data acquisition. The DSM had a 0.1 m resolution while the DEM was generated at 0.5 m and resampled to match DSM resolution. Canopy Height Models (CHM) were calculated using the difference between the DSM and the DEM (Li et al., 2020), as given in Equation 1 below which were validated with actual plant height measurements.

$$CHM = DSM - DEM , \quad (1)$$

where, DSM = Digital Surface Model
 DEM = Digital Elevation Model
 CHM = Canopy Height Model

2.2.2 Canopy Cover: For canopy cover, classified point clouds were rasterized at 0.1 m resolution, and vegetation pixels identified by elevation thresholds of 0.30 m. Canopy cover percentage was calculated as the ratio of vegetation pixels to the total number of pixels (Lu et al., 2021).

$$Canopy Cover (\%) = \frac{No. of Vegetation Pixels}{No. of Pixels} * 100\% , \quad (2)$$

2.2.3 Vegetation Indices: Vegetation indices including the Normalized Difference Vegetation Index (NDVI) Normalized Difference Yellowness Index (NDYI), Enhanced Vegetation Index (EVI), Chlorophyll Index - Red Edge (CI_{RedEdge}), Normalized Difference Red Edge Index (NDRE), Green Normalized Difference Vegetation Index (GNDVI) were calculated from the georeferenced PlanetScope imagery which were then processed for extraction on VIs in Google Earth Engine.

$$NDVI = \frac{NIR - R}{NIR + R} , \quad (3)$$

$$NDYI = \frac{G - B}{G + B} , \quad (4)$$

$$EVI = \frac{G - B}{G + B} , \quad (5)$$

$$CI_{RedEdge} = \frac{G - B}{G + B} , \quad (6)$$

$$NDRE = \frac{G - B}{G + B} , \quad (7)$$

$$GNDVI = \frac{G - B}{G + B} , \quad (8)$$

where R = Red (Band 6)
 G = Green (Band 4)
 B = Blue (Band 2)
 NIR = Near-Infrared (Band 8)
 RE = Red Edge Band (Band 7)

2.3 Model Development & Validation

To obtain the different AGB estimation models, the two rice cultivars were separated due to phenological differences. Linear regression was performed to relate rice aboveground biomass (AGB) with individual remote sensing parameters. Multiple Linear Regression (MLR) was performed to incorporate both structural and spectral variables, with Pearson correlation and Variance Inflation Factor (VIF) used to select predictors and avoid multicollinearity (Kelly, 2025). Typically, a VIF value exceeding 10 suggests significant collinearity, indicating that the parameter should be removed with others to ensure the interpretability of the model.

Model validation process used Leave-One-Out Cross Validation (LOOCV) due to limited sample size, wherein $n=15$ for each rice cultivar, computing R^2 , RMSE, and relative RMSE (rRMSE) (Ma et al., 2023). The corrected Akaike Information Criterion (AICc) was also used to balance model fit and complexity, helping identify the best model per cultivar, with $\Delta AICc < 2$, which corresponds to the difference between AICc values of models from the minimum AICc, indicates statistical equivalence (Aabeyir et al., 2020; Akpa and Unuabonah, 2011).

3. Results and Discussion

3.1 LiDAR - Derived Structural Parameters and Rice Aboveground Biomass

This section presents the results for rice AGB estimation using the structural parameters derived from LiDAR data. Furthermore, this discusses the implications of the utilization of canopy height and canopy cover for aboveground biomass estimation from regression analysis.

3.1.1 Canopy Height: Figure 3 shows the CHMs for each rice variety across the data acquisition sessions. For NSIC Rc 160, the regression equation ($y = 606.89x - 36.173$) yielded an R^2 of 0.3362, indicating a moderate correlation and suggesting that other factors may also influence biomass. In contrast, NSIC Rc 222 showed a stronger relationship ($y = 827.07x - 229.6$, $R^2 = 0.7315$), with a steeper slope, indicating higher sensitivity of AGB to canopy height and stronger predictive potential.

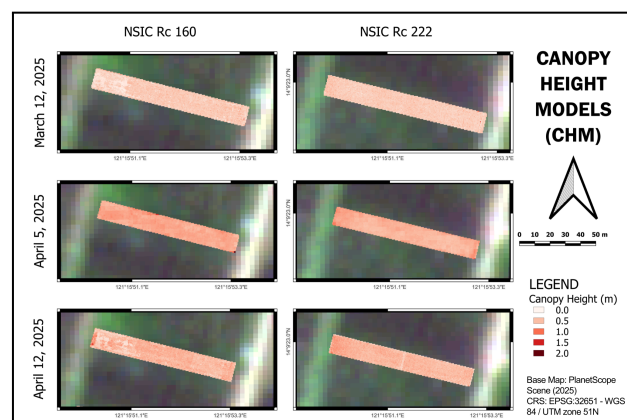


Figure 3. Extracted LiDAR Canopy Height Models

3.1.2 Canopy Height: Figure 4 shows the canopy cover (%) for each rice variety across the different data acquisition sessions. Both rice varieties showed a positive linear trend, with similar slopes (4.51 for Rc 222 and 4.61 for Rc 160), indicating comparable biomass gain per unit increase in canopy cover. NSIC Rc 222 had a stronger correlation ($R^2 = 0.6764$) than Rc 160 ($R^2 = 0.40$), suggesting canopy cover is a more reliable AGB predictor for Rc 222.

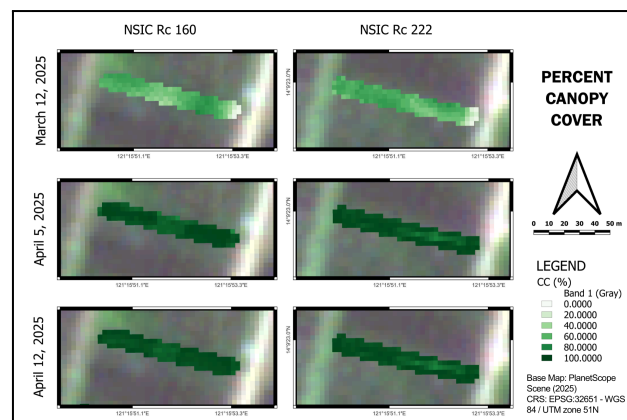


Figure 4. Extracted LiDAR Canopy Cover

3.2 PlanetScope - Derived Spectral Parameters and Rice Aboveground Biomass

The Normalized Difference Vegetation Index (NDVI), one of the most widely used vegetation indices for vegetation health, was evaluated for its relationship with rice aboveground biomass (AGB) using PlanetScope imagery. The analysis showed a positive linear relationship between NDVI and AGB for both NSIC Rc 222 and NSIC Rc 160 rice varieties. NSIC Rc 222 exhibited a stronger correlation, with an R^2 value of 0.4862, indicating that approximately 48.62% of the variation in AGB could be explained by NDVI. In contrast, NSIC Rc 160 showed a moderate correlation, with an R^2 value of 0.3907. These findings suggest that while NDVI is a useful indicator for biomass estimation its predictive strength may be improved with cultivar-specific calibration or additional variables.

The Normalized Difference Yellowness Index (NDYI), which captures reflectance in the yellow spectral region and can indicate plant maturity or stress, also showed a cultivar-dependent performance. For NSIC Rc 222, NDYI demonstrated a moderate positive relationship with AGB, with an R^2 value of 0.45. This indicates that NDYI could serve as a useful parameter for biomass estimation in this variety. However, for NSIC Rc 160, the correlation was weak and negative, with an R^2 of only 0.11, suggesting that NDYI had little to no predictive capability for this cultivar and may not be reliable during early growth stages.

The Enhanced Vegetation Index (EVI) showed very low correlation with AGB for both varieties. For NSIC Rc 222 and NSIC Rc 160, R^2 values were 0.04 and 0.0008 respectively, indicating that EVI explained less than 5% of the variability in AGB. This implies EVI may not be an effective index for estimating biomass in these rice cultivars under the study conditions.

Similarly, the Chlorophyll Index - Red Edge ($CI_{RedEdge}$), which is sensitive to chlorophyll content, showed very weak relationships with AGB. For NSIC Rc 222, the R^2 was nearly zero (0.00003), with a negative slope suggesting a non-significant or possibly erroneous relationship. NSIC Rc 160 performed slightly better with an R^2 of 0.16, but this still reflects a weak correlation, suggesting $CI_{RedEdge}$ is not a reliable indicator for biomass estimation in rice.

The Normalized Difference Red Edge Index (NDRE), which uses red-edge and near-infrared bands, also showed weak relationships with AGB. For NSIC Rc 222, the R^2 value was nearly zero (0.00009), while NSIC Rc 160 had a slightly better, yet still weak, correlation ($R^2 = 0.17$). These results suggest that NDRE is also not suitable for biomass estimation for either cultivar.

In contrast, the Green Normalized Difference Vegetation Index (GNDVI), derived from the green and NIR bands, showed the strongest performance among the indices tested. For NSIC Rc 222, the R^2 value was 0.51, indicating that over 50% of the AGB variation could be explained by GNDVI. For NSIC Rc 160, the correlation was even stronger, with an R^2 value of 0.62. Positive trends in both cultivars support the potential of GNDVI as a reliable, non-destructive parameter for rice AGB estimation.

3.3 Fusion of Spectral and Structural Parameters

This section focuses on the fusion of spectral and structural parameters derived from the multispectral imagery and LiDAR data, respectively. Moreover, this section presents the multicollinearity tests results of the parameters using statistical metrics, as well as, validation results to determine the best model for rice AGB estimation for the two rice cultivars.

3.3.1 Multicollinearity Measures: This section shows the results of the different metrics computed to assess the multicollinearity of the different rice parameters derived from LiDAR and multispectral data. In this section, rice cultivars were assessed to determine the correlation of the variables with each other and with the actual rice AGB data. Measures to prevent data redundancy are also discussed in this section for the model development of the rice AGB model.

3.3.1.1 NSIC Rc 160

	Variable	Correlation (r)	p-value
0	Canopy Height	0.5694	0.0267
1	Canopy Cover	0.6639	0.007
2	NDVI	0.6602	0.0074
3	NDYI	-0.1065	0.7057
4	EVI	0.0908	0.7476
5	$CI_{RedEdge}$	0.4845	0.0672
6	NDRE	0.4964	0.0599
7	GNDVI	0.8088	0.0003

Table 2. Correlation values and p-value of parameters for NSIC Rc 160 rice plot

For the NSIC Rc 160 variety, several parameters showed significant positive correlations with rice AGB, including Canopy Height ($r = 0.5694$, $p = 0.0267$), Canopy Cover ($r = 0.6639$, $p = 0.0070$), NDVI ($r = 0.6602$, $p = 0.0074$), and GNDVI ($r = 0.8088$, $p = 0.0003$), with GNDVI showing the strongest relationship. In contrast, NDYI and EVI had weak, non-significant correlations. $CI_{RedEdge}$ and NDRE showed moderate correlations but had p-values slightly above the 0.05 threshold. Thus, only the significantly correlated variables, namely Canopy Height, Canopy Cover, NDVI, and GNDVI, are suitable for model development, as shown in Table 2.

	Canopy Height	Canopy Cover	NDVI	GNDVI
Canopy Height	1			
Canopy Cover	0.7761	1		
NDVI	0.2730	0.4445	1	
GNDVI	0.5116	0.6768	0.8851	1

Table 3. Correlation Matrix for NSIC Rc 160 rice plot

The correlation matrix for NSIC Rc 160, as shown in Table 3, shows a strong relationship between Canopy Height and Canopy Cover while Canopy Cover and GNDVI also show moderate correlation, indicating potential redundancy and multicollinearity risk. Significantly, NDVI and GNDVI are highly correlated ($r=0.8851$), which signifies a strong collinearity, suggesting possible multicollinearity which may affect the model development. Hence, to address this the VIF was computed, as seen in Table 4. While both parameters have VIF values above the acceptable threshold, GNDVI demonstrates a stronger individual correlation with rice AGB ($r=0.7082$). GNDVI is retained in the model, while NDVI is excluded to reduce multicollinearity.

	R ²	VIF
NDVI	0.8357	6.0863
GNDVI	0.8873	8.8736
Canopy Height	0.6215	2.6423
Canopy Cover	0.7227	3.6064

Table 4. Variance Inflation Factors for NSIC Rc 222 rice plot

3.3.1.2 NSIC Rc 222

	Variable	Correlation (r)	p-value
0	Canopy Height	0.8544	0
1	Canopy Cover	0.8219	0.0002
2	NDVI	0.6975	0.0038
3	NDYI	0.6705	0.0062
4	EVI	0.1936	0.4894
5	CI _{RedEdge}	-0.0201	0.9433
6	NDRE	-0.007	0.9802
7	GNDVI	0.7082	0.0031

Table 5. Correlation values and p-value of parameters for NSIC Rc 222 rice plot

For NSIC Rc 222, correlation analysis revealed stronger relationships between parameters with rice AGB, as shown in Table 5, in comparison to results for Rc 160. Canopy Height and Canopy Cover showed very strong, significant correlations, while NDVI, GNDVI, and NDYI were also strongly and significantly correlated. In contrast, EVI, CI_{RedEdge}, and NDRE showed weak or no correlations ($p > 0.05$) and are not recommended for modeling. Overall, Canopy Height, Canopy Cover, NDVI, NDYI, and GNDVI are the most promising parameters for AGB estimation in Rc 222.

Table 6 shows the correlation matrix for NSIC Rc 222, wherein strong correlations were observed among independent parameters, suggesting possible multicollinearity. Canopy Height and Canopy Cover ($r=0.8094$), NDVI and GNDVI ($r=0.8666$), and NDVI and NDYI ($r=0.7580$) may reflect overlapping information.

	Canopy Height	Canopy Cover	NDVI	NDYI	GNDVI
Canopy Height	1				
Canopy Cover	0.8094	1			
NDVI	0.6478	0.4047	1		
NDYI	0.6031	0.5995	0.7578	1	
GNDVI	0.5490	0.3933	0.8666	0.5570	1

Table 6. Correlation Matrix for NSIC Rc 222 rice plot

Table 7 shows that NDVI had the highest VIF (12.24), exceeding the threshold of 10, indicating strong multicollinearity. Canopy Height and Canopy Cover showed moderate multicollinearity, but Canopy Height was retained due to its stronger correlation with biomass. Thus, NDVI and Canopy Cover were excluded, while Canopy Height, GNDVI, and NDYI were retained for model reliability.

	R ²	VIF
Canopy Height	0.819999	5.555512
Canopy Cover	0.810142	5.26709
NDVI	0.918333	12.24487
NDYI	0.774693	4.438386
GNDVI	0.816922	5.46216

Table 7. Variance Inflation Factors for NSIC Rc 222 rice plot

3.3.2 Multiple Linear Regression: Six AGB estimation models were developed per rice variety using selected spectral, structural, and data fusion parameters. Parameter selection was guided by correlation analysis and VIF results to minimize multicollinearity and improve model stability.

As summarized in Table 8 and visualized in Figures 5 to 10, model performance varied across parameter types and rice varieties.

Data Type	Parameters	R ²	RMSE (g)	rRMSE (%)
NSIC Rc 160				
Spectral (GNDVI)	y = -2225.41 +3809.67x	0.62	5.16	1.85
Structural (Canopy Height & Canopy Cover)	y = -114.82 + 223.00x ₁ + 3.36x ₂	0.41	103.19	37.05
Data Fusion (GNDVI, Canopy Height, & Canopy Cover)	y = -1911.59 + 3113.81x ₁ + 181.24x ₂ + 0.60x ₃	0.65	9.79	3.51
NSIC Rc 222				
Spectral (NDYI & GNDVI)	y = -1789.72 + 1598.04x ₁ + 2934.80x ₂	0.62	38.07	21.45
Structural (Canopy Height)	y = -229.59 + 827.06x	0.73	17.05	9.61
Data Fusion (NDYI, GNDVI, & Canopy Height)	y = -1258.281 + 559.83x ₁ + 1782.83x ₂ + 582.820x ₃	0.82	10.39	5.86

Table 8. Summary of Rice AGB Estimation Models and Performance Metrics

For NSIC Rc 160, the spectral model using GNDVI performed best, achieving an R² of 0.62 and the lowest rRMSE of 1.85%. The structural model, using canopy height and canopy cover, showed the weakest performance (R² = 0.41, rRMSE = 37.05%), while the fusion model moderately improved accuracy (R² = 0.65, rRMSE = 3.51%).

For NSIC Rc 222, the data fusion model combining NDVI, GNDVI, and canopy height yielded the best performance overall, with an R^2 of 0.82, RMSE of 10.39 g, and the lowest rRMSE of 5.86%. The structural model followed with an R^2 of 0.73 and rRMSE of 9.61%, while the spectral model showed higher error levels (rRMSE = 21.45%).

These results emphasize the advantage of data fusion models, which consistently outperformed single-parameter models by capturing complementary information from both structural and spectral domains, leading to more accurate rice AGB prediction.

In the following Figures 5 to 10, the AGB estimates from the parameters combinations and utilizing Multiple Linear Regression, per rice cultivar are shown for visualization of the ability of each of the models to estimate rice AGB. Figure 5 shows the spatial distribution of rice AGB generated using the spectral model for NSIC Rc 160, with GNDVI as the predictor. The map highlights relatively uniform estimates across the field, reflecting GNDVI's capacity to capture vegetation vigor.

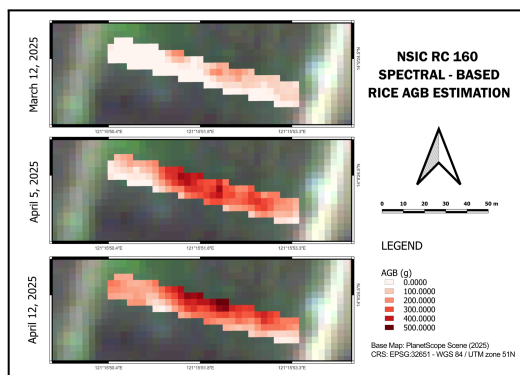


Figure 5. NSIC Rc 160 Spectral-Based AGB Estimation

Figure 6 presents the structural model for NSIC Rc 160, derived from canopy height and canopy cover. The map shows greater variability in biomass distribution, with some areas underestimated compared to field conditions.

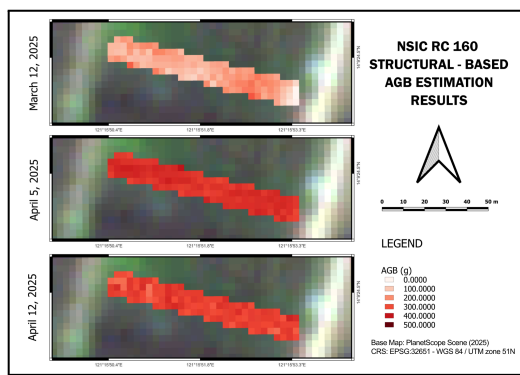


Figure 6. NSIC Rc 160 Structural-Based AGB Estimation

Figure 7 illustrates the data fusion model for NSIC Rc 160, integrating GNDVI, canopy height, and canopy cover. The resulting AGB map displays improved differentiation across plots, with better representation of biomass variation compared to the structural model.

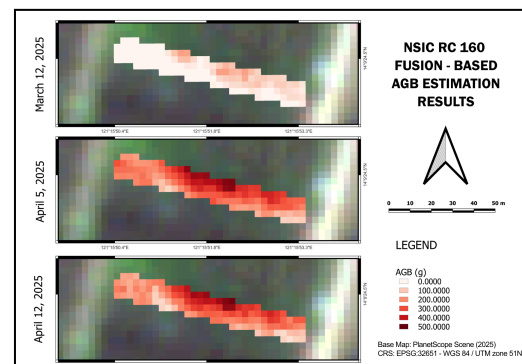


Figure 7. NSIC Rc 160 Fusion-Based AGB Estimation

Figure 8 shows the spectral model for NSIC Rc 222, combining NDVI and GNDVI. The spatial map indicates inconsistent biomass predictions across the field, with patches of overestimation and underestimation.

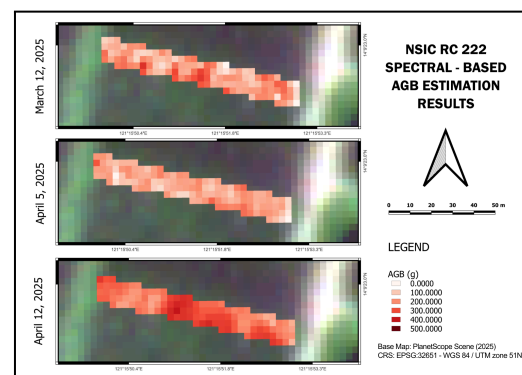


Figure 8. NSIC Rc 222 Spectral-Based AGB Estimation

Figure 9 displays the structural model for NSIC Rc 222, based solely on canopy height. The AGB map shows a clearer spatial gradient that aligns more closely with observed field biomass.

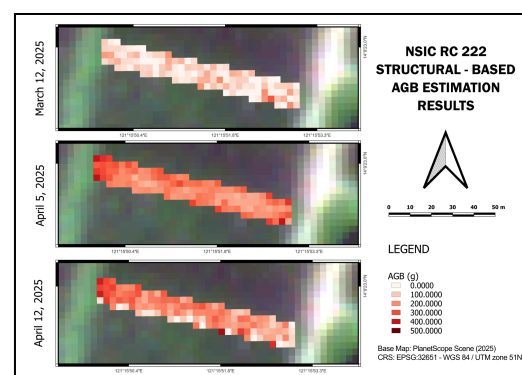


Figure 9. NSIC Rc 222 Structural-Based AGB Estimation

Figure 10 presents the data fusion model for NSIC Rc 222, integrating NDVI, GNDVI, and canopy height. The spatial distribution map demonstrates the most consistent and realistic biomass patterns, minimizing both underestimation and overestimation.

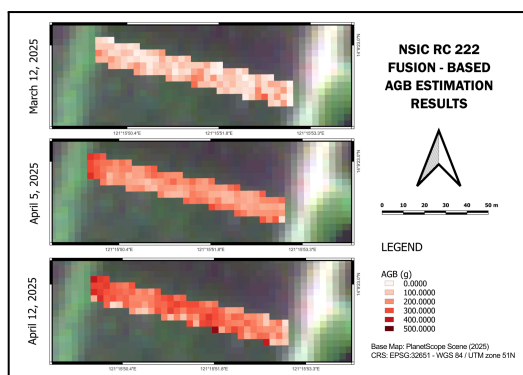


Figure 10. NSIC Rc 222 Fusion-Based AGB Estimation

3.3.3 Model Validation: This section presents the results of model validation using Leave-One-Out Cross Validation (LOOCV) to minimize bias and overfitting, given the limited sample size. For each rice variety, three models, the spectral-only, structural-only, and data fusion, were developed. The corrected Akaike Information Criterion (AICc) was also computed to support model selection. Table 9 summarizes the performance metrics of the regression models for rice AGB estimation.

Data Type	Parameters	R ²	RMSE (g)	rRMSE (%)
NSIC Rc 160				
Spectral (GNDVI)	$y = -2225.41 + 3809.67x$	0.51	124.30	47.05
Structural (Canopy Height & Canopy Cover)	$y = -114.82 + 223.00x_1 + 3.36x_2$	0.07	171.08	64.76
Data Fusion (GNDVI, Canopy Height, & Canopy Cover)	$y = -1911.59 + 3113.81x_1 + 181.24x_2 + 0.60x_3$	0.33	146.09	55.30
NSIC Rc 222				
Spectral (NDVI & GNDVI)	$y = -1789.72 + 1598.04x_1 + 2934.80x_2$	0.33	146.09	55.30
Structural (Canopy Height)	$y = -229.59 + 827.06x$	0.36	78.83	44.19
Data Fusion (NDVI, GNDVI, & Canopy Height)	$y = -1258.281 + 559.83x_1 + 1782.83x_2 + 582.820x_3$	0.64	58.87	33.00

Table 9. Summary of Rice AGB Estimation Models and Performance Metrics After Leave One Out Cross Validation

Table 10 presents the AICc values used to assess model fit and complexity. Alongside RMSE, rRMSE, and R², these values help identify the most effective model for estimating rice AGB per variety.

Data Type	AICc	Δ AICc
NSIC Rc 160		
Spectral (GNDVI)	187.10	0
Structural (Canopy Height & Canopy Cover)	197.29	10.19
Data Fusion (GNDVI, Canopy Height, & Canopy Cover)	192.49	5.39
NSIC Rc 222		
Spectral (NDVI & GNDVI)	174.21	8.61
Structural (Canopy Height)	165.60	0
Data Fusion (NDVI, GNDVI, & Canopy Height)	166.29	0.69

Table 10. Results of corrected Akaike Information Criterion (AICc) for Rice AGB Estimation Models

For NSIC Rc 160, the spectral-only model using GNDVI performed best, with consistent results across LOOCV (R² = 0.51, RMSE = 124.30, rRMSE = 47.05%) and independent validation. It also had the lowest AICc (187.10), confirming its suitability. Structural and data fusion models showed weaker performance and higher AICc values, suggesting added parameters did not improve accuracy and introduced noise.

In contrast, NSIC Rc 222 benefited from structural data. The structural-only model had improved LOOCV results (R² = 0.64, RMSE = 58.87, rRMSE = 33.00%) and the lowest AICc (165.60). The data fusion model had the best overall metrics (R² = 0.66, RMSE = 57.56, rRMSE = 32.27%) and was consistent with independent validation, despite a slightly higher AICc (166.29). Since the ΔAICc between these two models was only 0.69, they are statistically equivalent in fit.

Overall, results indicate that spectral data alone suffices for NSIC Rc 160, as the spectral model already yielded high accuracy with minimal added value from structural data. This suggests that Rc 160's canopy characteristics may be more effectively captured through spectral responses such as vegetation indices.

In contrast, NSIC Rc 222 benefited significantly from the combination of both structural (LiDAR-derived) and spectral inputs, indicating that this variety's AGB variation is influenced by both canopy height and reflectance characteristics. The strong performance of the fusion model for Rc 222 highlights the importance of integrating LiDAR with multispectral imagery to better represent its biophysical traits.

The use of multiple evaluation metrics, including R^2 , RMSE, and rRMSE, alongside AICc, ensured balanced assessment of model quality. These insights emphasize the variety-specific applicability of structural and spectral features in AGB modeling, underlining the need to input selection based on crop characteristics.

4. Conclusion

This study developed AGB estimation models for NSIC Rc 160 and NSIC Rc 222 using UAV-based LiDAR structural data and PlanetScope spectral imagery. Three MLR models were built per variety: spectral-only, structural-only, and data fusion. Performance was assessed using LOOCV, independent validation, and AICc.

For NSIC Rc 160, the spectral-only model using GNDVI performed best, with R^2 values of 0.51 (LOOCV) and 0.62 (validation), and the lowest AICc (187.10). Structural parameters did not improve performance and introduced variability, confirming Rc 160's responsiveness to spectral data alone.

Conversely, Rc 222 benefited from structural input. The structural-only model achieved $R^2 = 0.64$, while the data fusion model reached $R^2 = 0.66$ (LOOCV) and 0.82 (validation), with the lowest RMSE and rRMSE. Though the structural-only model had a slightly lower AICc, the small Δ AICc (0.69) indicates both models fit similarly well.

While the models were calibrated for specific varieties and conditions, they offer a framework for AGB estimation that can be adapted with local data. Due to the limited sample size, LOOCV was used, though larger datasets in future studies could allow for better generalization and the use of advanced models like Random Forest.

In summary, MLR models using LiDAR and satellite data effectively estimate rice AGB in a variety-sensitive way: Rc 160 favors spectral-only models, while Rc 222 performs better with combined inputs. These models have potential for precision agriculture and yield forecasting, especially if expanded with more variables and seasonal data.

Acknowledgements

We would like to extend our sincere gratitude to all who contributed to the successful completion of this study. We acknowledge Precision Path Technologies Inc., particularly Mr. Lowell Sy, for providing LiDAR data and financial assistance. We also thank the agricultural experts from the University of the Philippines Los Baños, namely Dr. Pompe Sta. Cruz, Dr. Moises Dorado, Dr. Crisanta Bueno, and Mr. Enrique Monserrat, for their support in fieldwork and technical advice. We are grateful to the Department of Science and Technology Science Education Institute for the thesis grant provided through the undergraduate scholarship program. Our heartfelt appreciation goes to our families, friends, and loved ones for their unwavering support.

References

Aabeyir, R., Adu-Bredu, S., Agyare, W.A., Weir, M.J.C., 2020. Allometric models for estimating aboveground biomass in the tropical woodlands of Ghana, West Africa. *Forest Ecosystems*. doi.org/10.1186/s40663-020-00250-3.

Akpa, O., Unuabonah, E., 2023. Small-Sample Corrected Akaike Information Criterion: An appropriate statistical tool for ranking of adsorption isotherm models. *Desalination*. doi.org/10.1016/j.desal.2010.12.057.

Fukagawa, N. K., Ziska, L. H., 2019. Rice: Importance for Global Nutrition. *Journal of nutritional science and vitaminology*. doi.org/10.3177/jnsv.65.S2

Kelly, R.C., 2025. *Variance Inflation Factor (VIF)*. Investopedia. www.investopedia.com/terms/v/variance-inflation-factor.asp

Khodjaev, S., Kuhn, L., Bobjonov, I., Glauben, T., 2023. Combining multiple UAV-Based indicators for wheat yield estimation, a case study from Germany. *European Journal of Remote Sensing*, 57(1). doi.org/10.1080/22797254.2023.2294121

Li, P., Zhang, X., Wang, W., Zheng, H., Yao, X., Tian, Y., Zhu, Y., Cao, W., Chen, Q., Cheng, T., 2020. Estimating aboveground and organ biomass of plant canopies across the entire season of rice growth with terrestrial laser scanning. *International Journal of Applied Earth Observation and Geoinformation*. doi.org/10.1016/j.jag.2020.102132.

Lu, J., Cheng, D., Geng, C., Zhang, Z., Xiang, Y., Hu, T., 2021. Combining plant height, canopy coverage and vegetation index from UAV-based RGB images to estimate leaf nitrogen concentration of summer maize. *Biosystems Engineering*. doi.org/10.1016/j.biosystemseng.2020.11.010.

Ma, J., Zhang, W., Ji, Y., Huang, J., Huang, G., Wang, L., 2023. Total and component forest aboveground biomass inversion via LiDAR-derived features and machine learning algorithms. *Front. Plant Sci.* doi: 10.3389/fpls.2023.1258521

Mansaray, L.R., Zhang, K., Kanu, A.S., 2020. Dry biomass estimation of paddy rice with Sentinel-1A satellite data using machine learning regression algorithms. *Computers and Electronics in Agriculture*. doi.org/10.1016/j.compag.2020.105674

Ndikumana, E., Ho Tong Minh, D., Dang Nguyen, H. T., Baghdadi, N., Courault, D., Hossard, L., El Moussawi, I., 2018: Estimation of Rice Height and Biomass Using Multitemporal SAR Sentinel-1 for Camargue, Southern France. *Remote Sensing*, 10(9), 1394. doi.org/10.3390/rs10091394

Sergieieva, K., 2024. *Vegetation Indices To Drive Digital Agri Solutions*. EOS Data Analytics. eos.com/blog/vegetation-indices/

Wan, L., Cen, H., Zhu, J., Zhang, J., Zhu, Y., Sun, D., Du, X., Zhai, L., Weng, H., Li, Y., Li, X., Bao, Y., Shou, J., He, Y., 2020. Grain yield prediction of rice using multi-temporal UAV-based RGB and multispectral images and model transfer – a case study of small farmlands in the South of China. *Agricultural and Forest Meteorology*. doi.org/10.1016/j.agrformet.2020.108096.

Zheng, H., Cheng, T., Zhou, M., Li, D., Yao, X., Tian, Y., Cao, W., Zhu, Y., 2019: Improved estimation of rice aboveground biomass combining textural and spectral analysis of UAV imagery. *Precision Agriculture*, 20, 611–629. doi.org/10.1007/s11119-018-9600-7